IEEE Photonics Journal
An IEEE Photonics Society Publication

Open Access

Optical Absorption Characteristic in Thin a-Si Film Embedded Between an Ultrathin Metal Grating and a Metal Reflector

Volume 5, Number 5, October 2013

Sangjun Lee
Sangin Kim

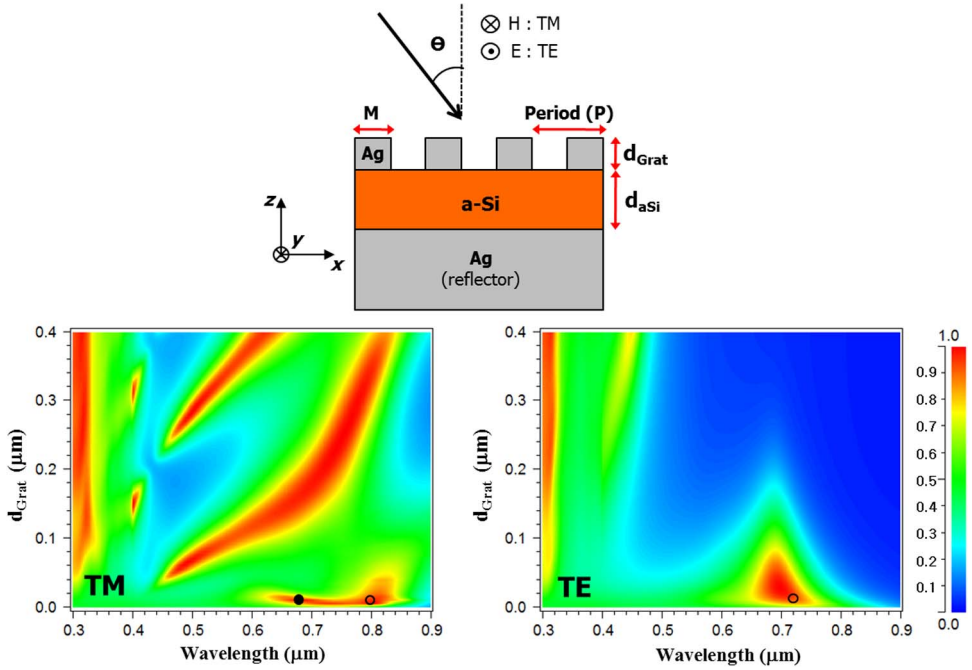

DOI: 10.1109/JPHOT.2013.2280339
1943-0655 © 2013 IEEE

IEEE photonics SOCIETY

IEEE

Optical Absorption Characteristic in Thin a-Si Film Embedded Between an Ultrathin Metal Grating and a Metal Reflector

Sangjun Lee[1] **and Sangin Kim**[2]

[1]Department of Electrical Engineering and Computer Science, Seoul National University, Seoul 151-742, Korea
[2]Department of Electrical and Computer Engineering, Ajou University, Suwon 443-749, Korea

DOI: 10.1109/JPHOT.2013.2280339

Manuscript received May 28, 2013; revised August 21, 2013; accepted August 21, 2013. Date of publication August 30, 2013; date of current version September 6, 2013. This work was supported by the National Research Foundation of Korea under Grants NRF-2011-0014265, NRF-2008-0662256, and NRF-2009-0094046. Corresponding author: S. Kim (e-mail: sangin@ajou.ac.kr).

Abstract: We numerically investigated the effect of an optically ultrathin top metal grating in an absorber structure composed of an amorphous silicon (a-Si) thin film and a metal reflector for efficient solar cells. The ultrathin metal grating-based structure shows nearly polarization-insensitive net absorption due to a great improvement for TE polarized wave, which is about 2.5 times enhanced compared with a relatively thick metal grating case. In particular, it is also shown that the absorption angle of the proposed solar cell is as wide as 80° owing to light coupling into an active layer through a leaky mode of flat dispersion characteristic for TM polarization.

Index Terms: Photovoltaic cell, leaky mode, metal grating, plasmonics.

1. Introduction

A fundamental limitation in solar cells in general is the trade-off between a longer optical length required for high photon absorption efficiency and a shorter electronic length required for faster diffusion of charge carriers. Thin film solar cell suffers from short optical length, but could efficiently reduce charge carrier recombination in an active layer. Therefore, developing the technology to efficiently trap light within the thin cell becomes the key issue in obtaining low cost, high efficiency solar cells viable for commercial production.

Recently, solar cell structures enhanced by surface plasmon polariton (SPP) or localized surface plasmon (LSP) via metallic nanostructure such as grating or nano-particle have been studied [1]–[4]. The associated absorption enhancement occurs due to strong field localization and resonantly enhanced field scattering near the metal-absorbing material interface [5]–[8]. However, this improvement scheme only works for TM polarized wave since in such structures, only TM wave is capable of exciting surface plasmon. In literature, solar cell structure optimized for TM wave often results in subpar performance for TE wave [9]–[11]. One may use two-dimensional nano-structuring to solve the aforementioned limitation, however, such structure comes at a cost of an expensive and complex fabrication process. Yang Wang *et al.* showed that a checkerboard patterned metal film and a thin absorber film can form a broadband superabsorber via negative refraction effect [12].

In this paper, we focus on reducing the polarization dependency of optical absorption efficiency and widening of absorption angle in a 1-D metal grating assisted thin a-Si film structure. From the finding that for both TM and TE waves, a leaky mode of a very flat-dispersion characteristic exists in

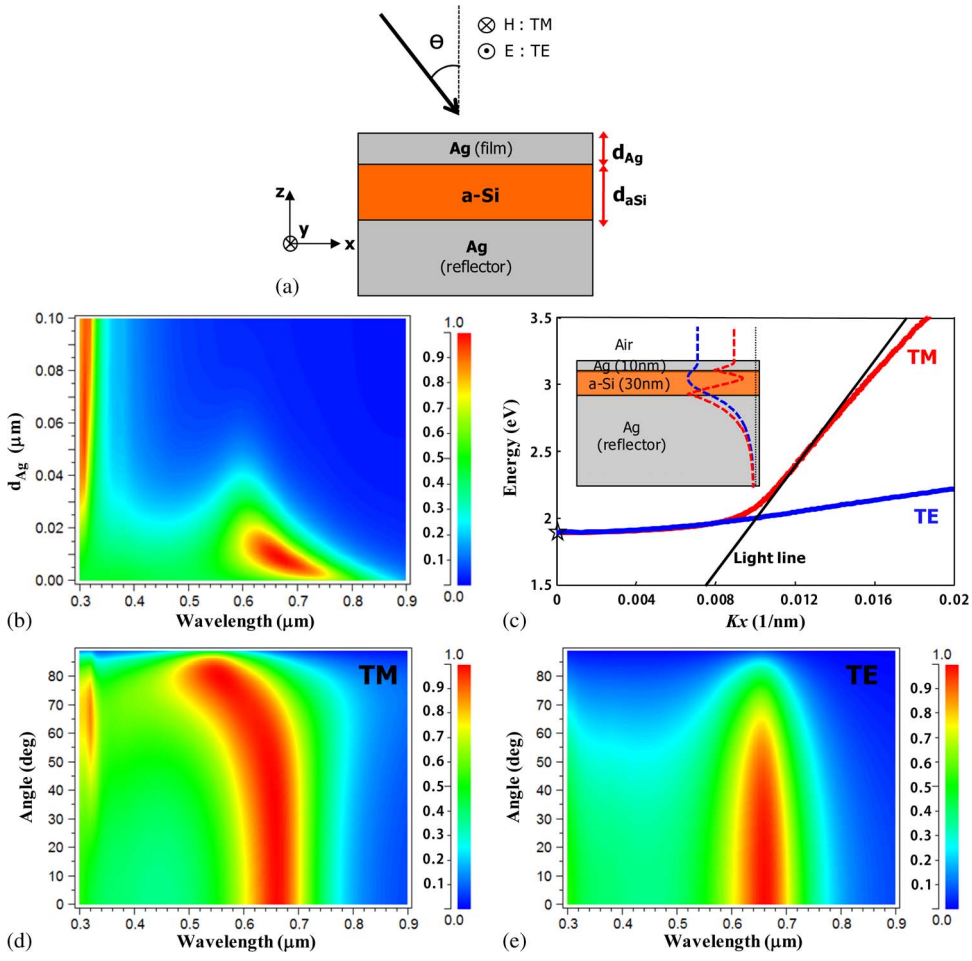

Fig. 1. (a) Geometry of absorber structure with flat top metal film. (b) Absorption efficiency spectra as a function of metal film thickness for $\theta = 0$. (c) Dispersion relation of fundamental TM and TE mode for a specific Ag/a-Si/Ag/Air structure with $d_{Ag} = 0.01$ μm and $d_{aSi} = 0.03$ μm. The amplitudes of magnetic field (H_y, red dashed) and electric field (E_y, blue dashed) of the mode at $\lambda = 0.658$ μm (indicated by black star) are shown in the inset, and black solid line corresponds to Air light line. Absorption efficiency spectra for (d) TM and (e) TE polarizations as a function of incident angle for the same structure depicted in (c).

the structure of a thin absorber sandwiched by an optically ultrathin flat metal film and a semi-infinite metal reflector, we propose an ultrathin metal grating based absorber structure for efficient solar cells. The effect of the metal grating thickness are investigated using rigorous coupled wave analysis (RCWA) based commercial software, DiffractMOD [13]. We demonstrate that the proposed absorber structure offers high performance over a wide range of incident angle for both polarizations, compared to thick grating case. Also, remarkable improvement of an estimated short-circuit current density under standard AM 1.5G illumination shows the potential for efficient thin film solar cell applications.

2. Light Absorption in Absorber Structure With an Ultrathin Metal Film

Before discussing characteristics of an ultrathin metal grating assisted thin absorber structure, we analyze the leaky-mode based optical absorption in an absorber structure with an optically ultrathin flat metal film which is shown in Fig. 1(a). A thin amorphous silicon (a-Si) layer is sandwiched by a top metal film and a semi-infinite metal reflector. Both metal regions are made of silver. Resonant cavity

modes [14] and increase of exciton lifetime [15] in the similar structure have been studied previously. In the structure of an embedded dielectric layer between two semi-infinite metals, omni-directional resonant coupling is possible if the thickness of the dielectric layer is specifically chosen [16]. In our study, we focused on the effect of the top metal thickness (d_{Ag}) on the leaky mode coupling behavior for a fixed a-Si layer thickness ($d_{aSi} = 0.03\ \mu$m).

Fig. 1(b) shows the absorption efficiency for normal incidence wave ($\theta = 0$) as a function of λ and d_{Ag}. The absorption efficiency is calculated using the RCWA method and extracted from the reflection spectrum as (1-reflection efficiency) because of the semi-infinite bottom metal reflector, and it includes the absorption in the metals as well. The estimation of the net absorption in the a-Si layer is discussed in Section 3.3, which reveals that most of the absorption occurs in the a-Si layer for an ultrathin top metal film. In the calculation, experimentally measured complex dielectric constants data [17] of the materials were used, and only the wavelength range of $0.3 \sim 0.9\ \mu$m where the sun has strong terrestrial irradiation is considered. One can see that absorption performance peaks for $d_{Ag} = 0.01\ \mu$m with a resonant wavelength of $\lambda = 0.66\ \mu$m and a bandwidth of $\sim$100 nm. For $d_{Ag} > 0.03\ \mu$m, most of light is reflected and strong absorption is observed only for short wavelengths ($\lambda < \sim 0.32\ \mu$m), which is mainly attributed to the dissipation in the top metal layer.

In order to understand the strong absorption for $d_{Ag} = 0.01\ \mu$m, the dispersion relations of the fundamental TM and TE modes are calculated analytically [18] and plotted in Fig. 1(c). Note that we assume lossless silver and only take into account the real part of wave vector (Kx) for the convenience of the mode calculation. (In the RCWA calculation, the metallic loss is included.) Above the light line, the dispersion curve becomes very flat, and the density of mode (DOM) gets remarkably large at $Kx = 0$ near $E = \sim$1.88 eV ($\lambda = 0.66\ \mu$m). This flat leaky mode characteristic explains the strong absorption for the normal incidence with the resonant peak of $\lambda = 0.66\ \mu$m. The inset in Fig. 1(c) shows a magnetic field profile ($|H_y|$) of TM mode and an electric field profile ($|E_y|$) of TE mode at $\lambda = 0.658\ \mu$m close to $Kx = 0$. One can see that the fundamental both modes are leaky toward the air. We have found that this field profiles are identical to the one observed in the RCWA calculation, which is not shown here.

We investigated the dependency of absorption efficiency on an incident angle for both polarizations, as plotted in Fig. 1(d) and (e). The structure with $d_{Ag} = 0.01\ \mu$m and $d_{aSi} = 0.03\ \mu$m, which corresponds to optimal condition in Fig. 1(b), was considered. For both TM and TE waves, the peak wavelengths show negligible shift as incident angle increases up to $\theta = 60^\circ$. This result is consistent with Fig. 1(c) and a direct evidence for a wide-angle absorption by leaky mode coupling [16] of the incident light. Absorption characteristics for TM and TE polarizations are different for $\theta > 60^\circ$. In the TM polarization case, the absorption spectrum keep a strong peak (almost 1) even at $\theta = 80^\circ$. Whereas, in the TE polarization case, the absorption peak decrease for $\theta > 60^\circ$. This seems to stem from the difference in mode profiles. As shown in the inset of Fig. 1(c), the TM mode profile shows a relatively higher portion of energy in the a-Si layer compared to the TE mode profile, which implies TM wave can be absorbed better than TE wave. This difference is intensified for a larger incidence angle somehow.

From this investigation, we can conclude that the thin top metal layer of a properly chosen thickness induces leaky modes with a remarkably flat dispersion characteristics and thus, this enhanced leaky mode coupling can be utilized to realize high performance absorber with enhanced efficiency and a wide absorption angle. Based on this, we can expect further absorption performance improvement by introducing a grating structure in the top metal layer since light scattering effect from the added grating may exist. Absorption behaviors in the top metal grating based absorber structures are investigated in the next section.

3. Effect of Metal Grating Thickness on Absorption Performance

Fig. 2(a) shows the structure of a metal grating assisted absorber structure, which is similar to previously studied structures in Ref. [9], [11]. In this paper, the performance of the absorber structure with an ultrathin metal grating is investigated in comparison with the one with a thick metal grating. For fair comparison, 0.03 μm thick a-Si is used, which is the same as in Ref. [9], [11].

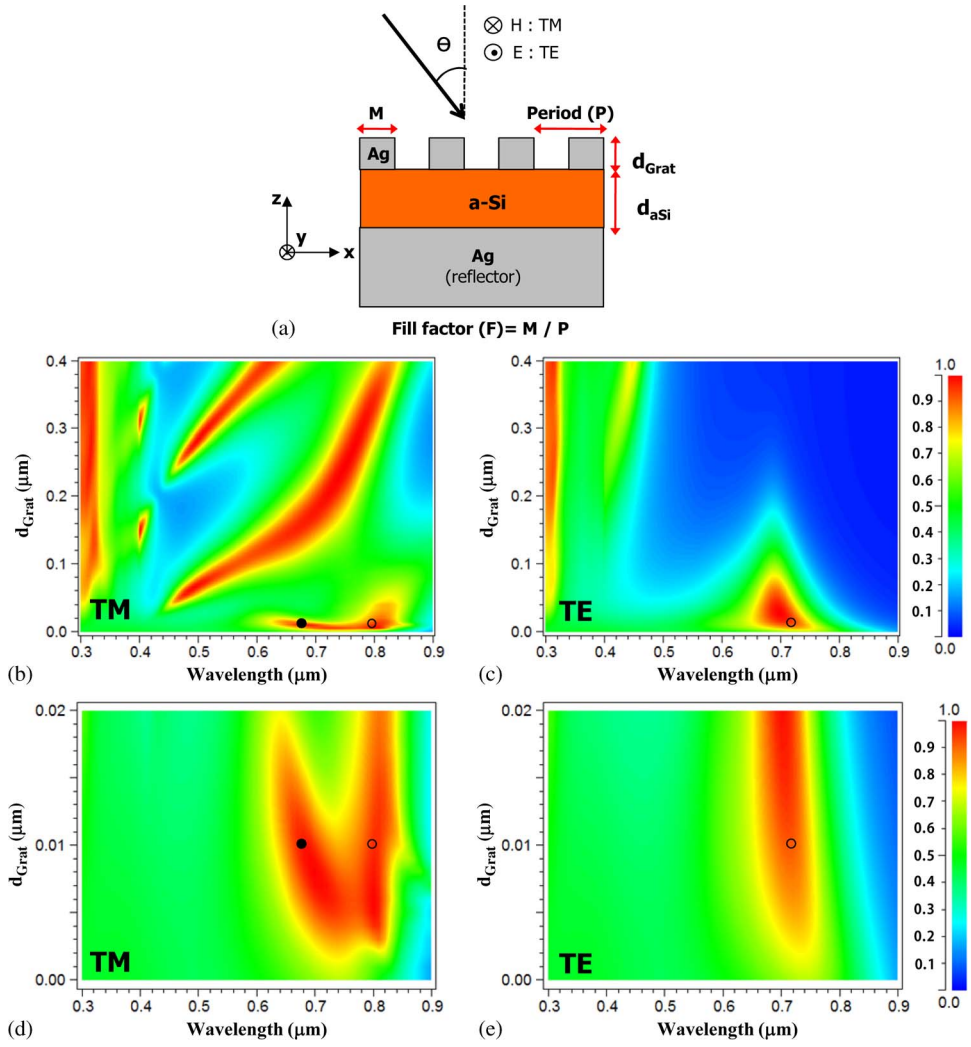

Fig. 2. (a) Geometry of absorber structure with metal grating. Absorption efficiency spectra for (b) TM and (c) TE polarization as a function of d_{Grat}. Two bottom plots (d) and (e) correspond to close-up of (b) and (c) to clarify for ultrathin grating case, respectively. In all calculations, $P = 0.4\ \mu$m, $F = 0.5$, $d_{aSi} = 0.03\ \mu$m, $\theta = 0$.

3.1. Polarization Dependence

The grating thickness dependence of absorption efficiency for normal incidence $(\theta = 0)$ is plotted in Fig. 2(b) and (c). Note that the period, the fill factor of the grating, the thickness of a-Si in this article are fixed to $P = 0.4\ \mu$m, $F = 0.5$, $d_{aSi} = 0.03\ \mu$m, respectively. When the top metal grating is relatively thick $(d_{Grat} > \sim 0.05\ \mu$m), various absorption peaks or dips for TM wave are observed, which can be attributed to Wood anomalies [19] and Fabry–Pérot (FP)-like resonances in the vertical direction within slit regions [20]. Two main absorption branches, which are associated with the FP-like resonance in the slit region, show red-shift with an increase of d_{Grat} as expected. Fig. 3(b) shows the field profile at the absorption peak wavelength $(\lambda = 0.56\ \mu$m) in an absorber structure with a thick metal grating of $d_{Grat} = 0.1\ \mu$m for TM wave. (This is the same structure considered in Ref. [9].) It is obvious that the main mechanism of the TM wave coupling into the a-Si layer is a waveguide effect of the slit segment of the grating [21]. While the metal grating of $d_{Grat} > \sim 0.05\ \mu$m supports relatively high absorption for TM wave, the absorption performance for TE wave is very poor as seen in Fig. 2(c). Fig. 3(c) shows the field profile in the same structure at the absorption peak wavelength $(\lambda = 0.69\ \mu$m) for TE wave, where a large portion of the incident

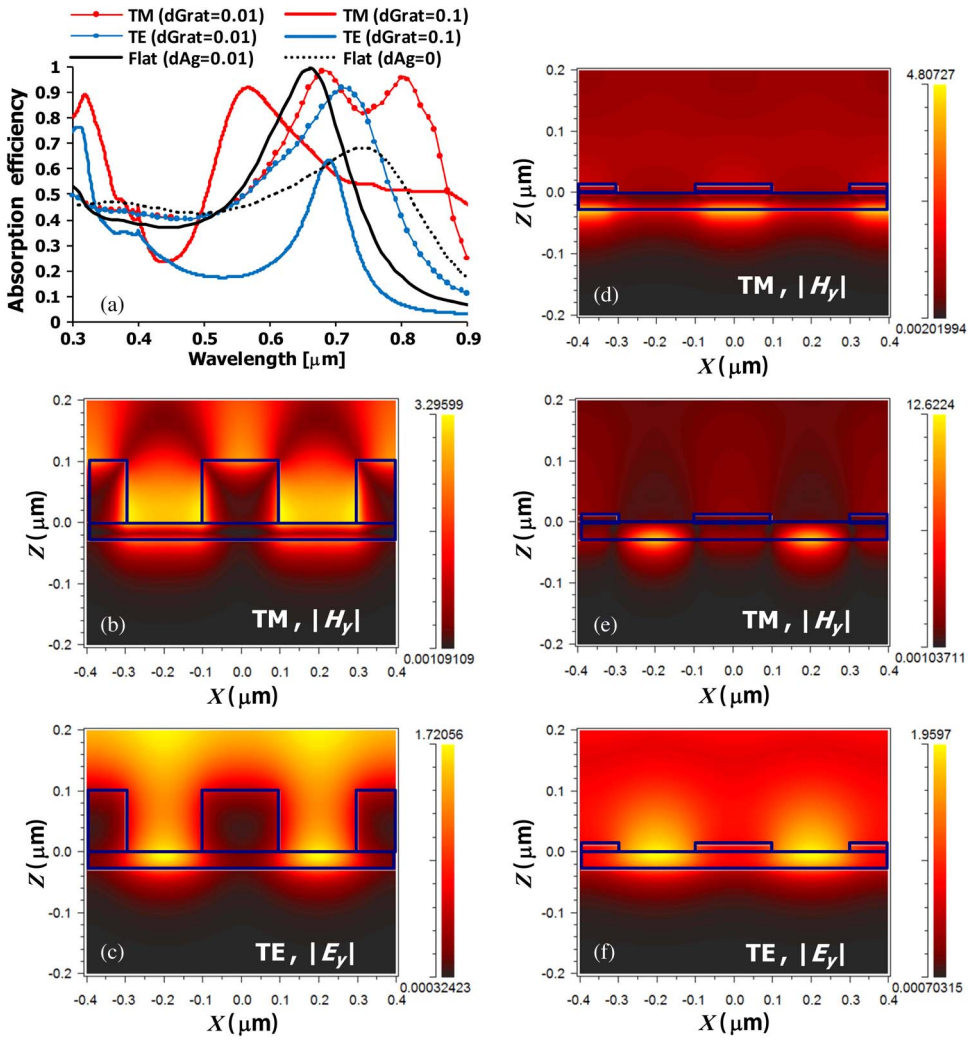

Fig. 3. (a) Absorption efficiency spectra for different grating thickness and polarization. The amplitude distribution of fields parallel to the grating at (b) $\lambda = 0.56$ μm for TM, (c) $\lambda = 0.69$ μm for TE in case of $d_{Grat} = 0.1$ μm, and at (d) $\lambda = 0.68$ μm, (e) $\lambda = 0.80$ μm for TM, (f) $\lambda = 0.72$ μm for TE in case of $d_{Grat} = 0.01$ μm (ultrathin grating). The parameters for plot (d) is marked by solid black circle in Fig. 2(d), and those for plot (e) and (f) are marked by open black circles in Fig. 2(d) and (e), respectively. In each field profiles, blue solid lines indicate the interfaces between different materials. In all calculations, amplitude of incident field components was set to 1 for both magnetic and electric field. $P = 0.4$ μm, $F = 0.5$, $d_{aSi} = 0.03$ μm, $\theta = 0$.

field is reflected. So, absorption performance of an absorber structure with thick grating is strongly dependent on polarization.

Whereas, in case of ultrathin grating ($d_{Grat} < 0.02$ μm), strong absorptions are observed for both polarizations as shown in Fig. 2(d) and (e). In Fig. 2(d), there are two absorption branches for TM wave. The left branch seems to stem from the leaky mode in the structure with an ultrathin flat top metal film. Fig. 3(d) shows the field profile at the left absorption peak wavelength ($\lambda = 0.68$ μm) in the absorber structure with an ultrathin metal grating of $d_{Grat} = 0.01$ μm for TM wave. One can see that the field is mainly localized in a-Si layer under the metal segment of the top grating and the field distribution along the vertical direction is quite similar to that in the structure with an ultrathin flat top metal [Fig. 1(c)]. The right absorption branch in Fig. 2(d) results from a localized surface plasmon excited by the scattering from the top metal grating structure. Fig. 3(e) shows the field profile at the right absorption peak ($\lambda = 0.80$ μm). One can see that the field is mostly confined in the slit

segment of the grating and the vertical field distribution is the same as a surface plasmon mode confined at the interface between the a-Si layer and the bottom semi-infinite metal. This surface plasmon mode is a guided mode and cannot be excited with a normal incident wave when the top ultrathin metal layer is flat. In the structure with the top metal grating, the surface plasmon mode can be excited via the guided-mode resonance phenomenon [22]. However, in our case, it seems that a incomplete guided-mode resonance occurs due to the week scattering strength of the ultrathin metal grating and the loss of the a-Si layer, and this is why more field is concentrated under the slit segment of the grating. For TE wave, there also is single strong absorption branch as seen in Fig. 2(e). Although the absorption peak wavelength is slightly different from that of the left absorption branch in the case of TM wave, the absorption for TE wave also seems to partially stem from the leaky mode in the structure with an ultrathin flat top metal film. Fig. 3(f) shows the field profile at the absorption peak wavelength ($\lambda = 0.72$ μm) in the absorber structure with an ultrathin metal grating of $d_{Grat} = 0.01$ μm for TE wave. In the metal segment of the grating, although field is less confined compared to the slit segment, the vertical field distribution is the same as that in the flat ultrathin grating structure depicted in the inset of Fig. 1(c) (the blue dashed curve). We surmise that the stronger field confinement in the slit segment is attributed to the scattering and loss of the metal as in the case of the longer wavelength absorption branch for TM wave. The effect of the ultrathin top grating is manifested by the comparison to the case of the thick top metal of $d_{Grat} = 0.1$ μm shown in Fig. 3(c). One can see that the reflection is greatly reduced in the case of the ultrathin grating due to the leaky mode property.

For more direct comparison, the absorption spectra for the ultrathin grating structure ($d_{Grat} = 0.01$ μm) are plotted with those for the thick grating structure ($d_{Grat} = 0.1$ μm) in Fig. 3(a). For references, the absorption spectra for the ultrathin flat metal structure and the structure without a top metal are also plotted. One can see that the TE wave absorption in the thick metal grating structure is even worse than that in the structure without a top metal. This implies that the thick metal grating works as a reflector for TE wave. In contrast to the thick metal grating, the ultrathin metal grating improves the absorption for both polarization and especially, more than twofold increase in overall absorption efficiency is achieved for TE wave. Our leaky mode based interpretation on the enhanced absorption in the ultrathin metal grating assisted absorber structure will be verified more by investigating the incident angle dependence in the next section.

3.2. Angle Dependence

Incident angle dependence of absorption is studied for the thick ($d_{Grat} = 0.1$ μm) and the ultrathin ($d_{Grat} = 0.01$ μm) grating structures. The thick grating structure has poor performances for oblique incidence, as shown in Fig. 4(a) and (b). For TM wave, absorption branches have quite narrow bandwidth and strongly depend on the incident angle. For example, the most strong absorption branch is located in the right side of the Wood-Rayleigh anomaly condition curve represented by a dashed black line in Fig. 4(a), that is, $\lambda = P(1 + \sin(\theta))$. For TE wave, although angle dependence of absorption for TE wave is weak, overall absorption efficiency is quite low, seen in Fig. 4(b).

For the ultrathin grating case, regardless of polarizations, the positions of the absorption peaks remain nearly constant up to $\theta = 60^\circ$ as shown in Fig. 4(c) and (d). For TM polarization, strong absorption is achieved up to $\theta = 80^\circ$. The left absorption branch for TM wave and single absorption branch for TE wave show very similar angle dependence as the ultrathin flat metal structure in Fig. 1(c) and (d). It seems that the Wood-Rayleigh anomaly condition does not affect the absorption in the ultrathin grating structure for both polarizations unlike the thick grating case, and the flat-dispersion leaky mode characteristic of the ultrathin flat metal film structure remains even after an introduction of grating structure to the ultrathin top metal layer.

3.3. Application to Solar Cells

So far, the calculated absorption efficiency includes the absorptions by a-Si and metal structures. Considering an application to solar cells, net absorption efficiency is accurately estimate by estimating the absorption by only a-Si since the absorption by the metal structures does not contribute

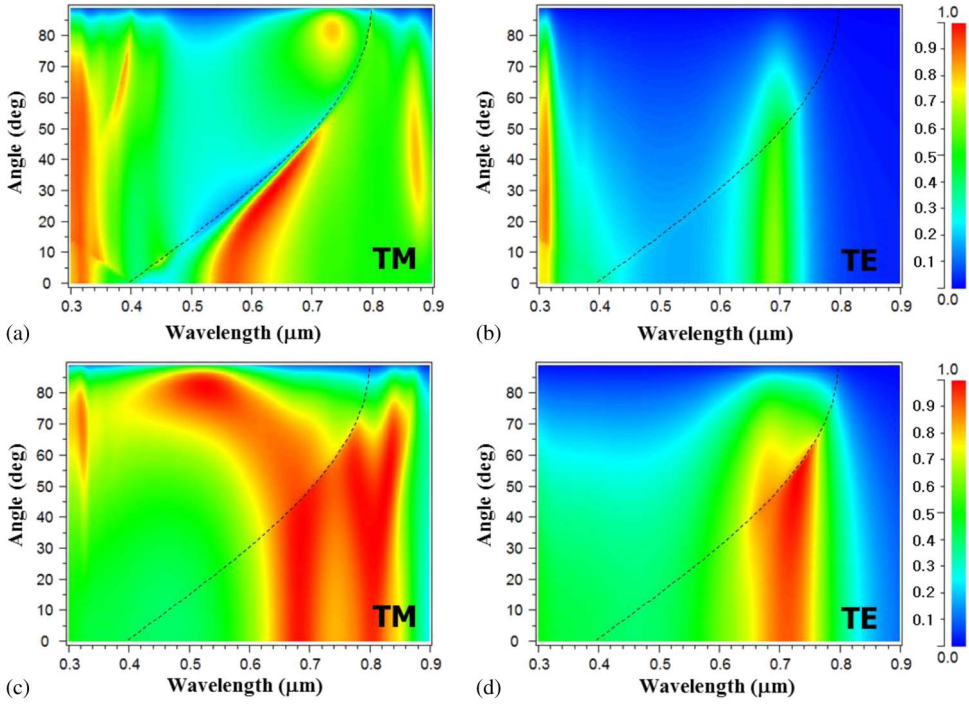

Fig. 4. Absorption efficiency spectra as a function of incident angle. Top panel: (a) TM and (b) TE polarization for $d_{Grat} = 0.1$ μm. Bottom panel: (c) TM and (d) TE polarization for $d_{Grat} = 0.01$ μm (ultrathin grating). In all calculations, $P = 0.4$ μm, $F = 0.5$, $d_{aSi} = 0.03$ μm. The dashed black lines correspond to Wood-Rayleigh anomaly condition.

to energy conversion. A portion of the absorption in a specific region of a unit cell can be determined by the ratio of integration of time-average power density (P_{ave}), which is defined as [11]

$$P_{ave} = \frac{\omega \cdot \mathrm{Im}(\varepsilon) \cdot |\vec{E}|^2}{2} \tag{1}$$

where ω is an excitation frequency, ε is dielectric constant of corresponding area, and E is electric field. Fig. 5 shows the portions of the absorptions by a-Si (red curves) and metal structures (green curves) separately. In all calculation, $P = 0.4$ μm, $F = 0.5$, $d_{aSi} = 0.03$ μm, $\theta = 0^\circ$ [These parameters are same as Fig. 3(a)]. For the ultrathin metal grating case of $d_{Grat} = 0.01$ μm, the difference between the both absorptions by a-Si for TM and TE polarizations is much smaller compared to the thicker grating case of $d_{Grat} = 0.1$ μm. Taking into account of solar irradiation, net absorption efficiency (A) is defined as

$$A = \frac{\int a(\lambda) \cdot S(\lambda) \cdot d\lambda}{\int S(\lambda) \cdot d\lambda} \tag{2}$$

where $a(\lambda)$ is absorption efficiency by a-Si, and $S(\lambda)$ is solar irradiance taken from Standard AM 1.5G. As indicated in Table 1, for both polarizations, the net absorption efficiencies of the ultrathin grating are improved compared to the thick grating case. Especially, for TE wave, huge enhancement of about 2.5 times is achieved. It is noteworthy that even the ultrathin flat metal structure outperforms the thick grating structure. We also estimated short-circuit current density (J_{sc}) defined as

$$J_{sc} = e \cdot \int_{300\,\mathrm{nm}}^{900\,\mathrm{nm}} \frac{\lambda}{h \cdot C_o} \cdot S(\lambda) \cdot a(\lambda) \cdot d\lambda \tag{3}$$

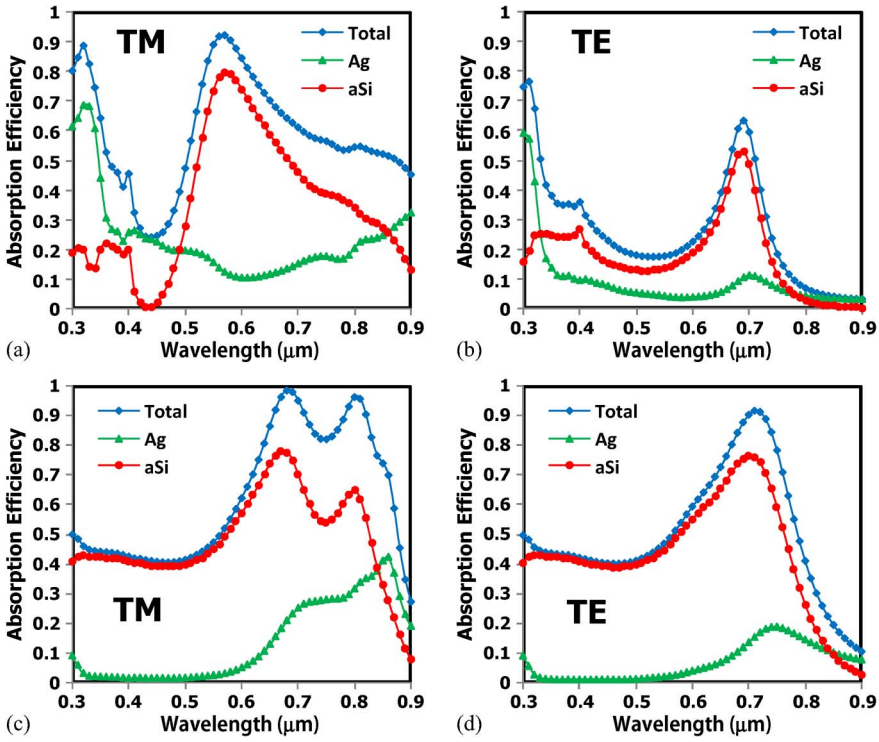

Fig. 5. Separation of absorption efficiencies in the proposed absorber structure. Top panel: (a) TM and (b) TE polarization for $d_{Grat} = 0.1$ μm. Bottom panel: (c) TM and (d) TE polarization for $d_{Grat} = 0.01$ μm (ultrathin grating). In all calculations, $P = 0.4$ μm, $F = 0.5$, $d_{aSi} = 0.03$ μm, $\theta = 0$.

TABLE 1

Net absorption efficiency and short-circuit current density (J_{sc})

	Flat Structure (d_{Ag}=0.01μm)	Ultrathin Grating (d_{Grat}=0.01μm)		Thick Grating (d_{Grat}=0.1μm)	
Polarization	Non-pol.	TM	TE	TM	TE
Total	0.485	0.637	0.520	0.590	0.241
Ag	0.080	0.135	0.069	0.188	0.060
a-Si	**0.405**	**0.502**	**0.451**	**0.402**	**0.181**
J_{sc} (mA/cm^2)	**12.94**	**16.94**	**14.83**	**13.59**	**5.88**

where h is Planck's constant, and C_o is light velocity in vacuum, assuming that each absorbed photon creates an electron-hole pair that gets collected without further losses. Due to the presence of interface defects between silicon and metal, recombination occurs and thus can degrade performance, but this effect is not considered here. So, our estimation may be the upper limit of the performance of our structure based solar cells. In spite of the ultrathin (30 nm) active layer, our estimated J_{sc} is comparable to $J_{sc} = 17$ mA/cm^2 of an excellent single junction a-Si solar cell with 250 nm thickness [23].

In order to realize solar cells based on the absorber structure considered in this work, a p-i-n junction should be formed for carrier extraction. The ultrathin active layer of 30 nm of our absorber structure may seem too thin to form a p-i-n junction. However, an a-Si solar cell of a 20 nm thick p-i-n (5 nm-10 nm-5 nm) junction has been experimentally demonstrated and it has been reported that the ultrathin nature of these junctions can lead to large internal electric fields, yielding reduced recombination and increased current [24].

As mentioned earlier, our choice of 30 nm thick a-Si layer is solely to clearly show the effect of the ultrathin metal grating in the fair comparison to the similar structure with a thick metal grating in Ref. [9],

[11]. So, the a-Si layer thickness can be changed for performance optimization with proper design of the top metal grating structure. In Ref. [12], even 15 nm thick a-Si layer based absorber structure was designed with a metamaterial concept and their theoretical analysis showed an excellent performance. Besides, in our absorber structure of 30 nm a-Si, absorption enhancement is achieved in a 700 $\sim$ 800 nm wavelength range and in a short wavelength range (300 $\sim$ 600 nm), our absorber structure suffers from relatively high reflection, which is due to high refractive index of the a-Si. Another issue about the absorption in the long wavelength range ($>$ 750 nm) in solar cells is a low carrier collection efficiency due to the localized characteristics of the tail state which governs the absorption. One simple solution to these problems is to reduce the a-Si layer for blue shift of the band edge of the leaky mode. From our calculation, it has been found that the absorption peak in the flat ultrathin metal structure is shifted to $\lambda = \sim$500 nm for $d_{aSi} = 0.015$ μm and $d_{Ag} = 0.01$ μm. Another possible way is to introduce additional low index layer such as ITO on top of the a-Si as in Ref. [12]. In both approaches, proper design of a metal grating structure is required to maintain the advantage of the leaky mode property of the ultrathin metal grating. Further optimization of our absorber structure for solar cells remains as a future work at this moment.

For a low-cost fabrication of the 10 nm thick Ag grating of 400 nm period over a wide area, a laser interference lithography and wet chemical etching can be used [25]. We have an experience to pattern 400 $\sim$ 500 nm periodic structure using the laser interference lithography. Metal gratings built with the wet chemical will have smooth edge. Since a sharp rectangular shape grating was assumed in our calculation, the performance of the built absorber will be rather different from our calculation. However, the difference may not be severe since the absorption in the ultrathin metal grating structure mainly stems from the leaky mode property of the flat thin metal structure and resonant characteristics of the grating does not play an important role in absorption enhancement. In realization of the absorber structure, another issue may be quality and optical property of 10 nm Ag film. Usually, metal films of $\sim$10 nm show much higher losses than bulk metals. Recently, it has been reported that the quality of ultra-thin Ag films ($<$ 10 nm) can be improve by using 1 nm thick Ge wetting layer during evaporation process and post annealing [26]. The measured optical properties of 6.5 nm thick Ag film were close to the bulk Ag over 400 $\sim$ 800 nm wavelength range.

4. Conclusion

In this paper, we have investigated the effect of ultrathin top metal grating in thin a-Si based absorber for efficient solar cells. By investigating the performance of a absorber structure with an ultrathin ($\sim$0.01 μm) flat top metal film properly chosen, we have found that strong absorption spectra are achieved over a wide range of incident angle up to $\theta = 80^\circ$ due to a leaky mode of flat-dispersion characteristic for TM polarization. We have also shown that the flat-dispersion leaky mode characteristic remains even when grating structure is introduced, and thus the performance of the solar cell can be further improved by the scattering from the grating. Net absorption in a thin a-Si layer of 0.03 μm with the ultrathin metal grating for TM is remarkably improved ($\sim$25%) compared to the structure with a thick ($\sim$0.1 μm) metal grating. Moreover, for TE polarization, approximately 2.5 times improvement is also achieved owing to a considerable decrease in reflection of incident light from top metal area via leaky mode coupling. As a result, the optically ultrathin metal grating has excellent behaviors for polarization-insensitive and wide-angle absorption.

References

[1] H. A. Atwater and A. Polman, "Plasmonics for improved photovoltaic devices," *Nat. Mater.*, vol. 9, no. 3, pp. 205–213, Mar. 2010.
[2] S. Pillai, K. R. Catchpole, T. Trupke, and M. A. Green, "Surface plasmon enhanced silicon solar cells," *J. Appl. Phys.*, vol. 101, no. 9, pp. 093105-1–093105-8, May 2007.
[3] K. R. Catchpole and A. Polman, "Design principles for particle plasmon enhanced solar cells," *Appl. Phys. Lett.*, vol. 93, no. 19, pp. 191113-1–191113-3, Nov. 2008.
[4] V. E. Ferry, J. N. Munday, and H. A. Atwater, "Design considerations for plasmonic photovoltaics," *Adv. Mater.*, vol. 22, no. 43, pp. 4794–4808, Sep. 2010.

[5] W. Wang, S. Wu, K. Reinhardt, Y. Lu, and S. Chen, "Broadband light absorption enhancement in thin-film silicon solar cells," *Nano Lett.*, vol. 10, no. 6, pp. 2012–2018, Jun. 2010.
[6] C. Pahud, V. Savu, M. Klein, O. Vazquez-Mena, F.-J. Haug, J. Brugger, and C. Ballif, "Stencil-nanopatterned back reflectors for thin-film amorphous silicon n-i-p solar cells," *IEEE J. Photovolt.*, vol. 3, no. 1, pp. 22–26, Jan. 2013.
[7] P. Zilio, D. Sammito, G. Zacco, M. Mazzeo, G. Gigli, and F. Romanato, "Light absorption enhancement in hetero-structure organic solar cells through the integration of 1-D plasmonic gratings," *Opt. Exp.*, vol. 20, no. S4, pp. A476–A488, May 2012.
[8] R. B. Dunbar, T. Pfadler, and L. Schmidt-Mende, "Highly absorbing solar cells—A survey of plasmonic nanostructures," *Opt. Exp.*, vol. 20, no. S2, pp. A177–A189, Mar. 2012.
[9] C.-C. Chao, C.-M. Wang, Y.-C. Chang, and J.-Y. Chang, "Plasmonic multilayer structure for ultrathin amorphous silicon film photovoltaic cell," *Opt. Rev.*, vol. 16, no. 3, pp. 343–346, May 2009.
[10] C. Min, J. Li, G. Veronis, J.-Y. Lee, S. Fan, and P. Peumans, "Enhancement of optical absorption in thin-film organic solar cells through the excitation of plasmonic modes in metallic gratings," *Appl. Phys. Lett.*, vol. 96, no. 13, pp. 133302-1–133302-3, Mar. 2010.
[11] C.-C. Chao, C.-M. Wang, and J.-Y. Chang, "Spatial distribution of absorption in plasmonic thin film solar cells," *Opt. Exp.*, vol. 18, no. 11, pp. 11 763–11 771, May 2010.
[12] Y. Wang, T. Sun, T. Paudel, Y. Zhang, Z. Ren, and K. Kempa, "Metamaterial-plasmonic absorber structure for high efficiency amorphous silicon solar cells," *Nano Lett.*, vol. 12, no. 1, pp. 440–445, Jan. 2012.
[13] M. G. Moharam, E. B. Grann, D. A. Pommet, and T. K. Gaylord, "Formulation for stable and efficient implementation of the rigorous coupled-wave analysis of binary gratings," *J. Opt. Soc. Amer. A, Opt. Image Sci.*, vol. 12, no. 5, pp. 1068–1076, May 1995.
[14] F. Villa, T. Lopez-Rios, and L. E. Regalado, "Electromagnetic modes in metal-insulator-metal structures," *Phys. Rev. B, Condens. Matter*, vol. 63, no. 16, pp. 165103-1–165103-4, Apr. 2001.
[15] L. T. Vuong, G. Kozyreff, R. Betancur, and J. Martorell, "Cavity-controlled radiative recombination of excitons in thin-film solar cells," *App. Phys. Lett.*, vol. 95, no. 23, pp. 233106-1–233106-3, Dec. 2009.
[16] H. Shin, M. F. Yanik, S. H. Fan, R. Zia, and M. L. Brongersma, "Omnidirectional resonance in a metal–dielectric–metal geometry," *Appl. Phys. Lett.*, vol. 84, no. 22, pp. 4421–4423, May 2004.
[17] E. D. Palik, *Handbook of Optical Constants of Solids*. New York, NY, USA: Academic, 1985.
[18] E. N. Economou, "Surface plasmons in thin films," *Phys. Rev.*, vol. 182, no. 2, pp. 539–554, Jun. 1969.
[19] R. W. Wood, "Anomalous diffraction gratings," *Phys. Rev.*, vol. 48, no. 12, pp. 928–936, Dec. 1935.
[20] X. Jiao, P. Wang, L. Tang, Y. Lu, Q. Li, D. Zhang, P. Yao, H. Ming, and J. Xie, "Fabry–Pérot-like phenomenon in the surface plasmons resonant transmission of metallic gratings with very narrow slits," *Appl. Phys. B*, vol. 80, no. 3, pp. 301–305, Mar. 2005.
[21] S. Collin, F. Pardo, R. Teissier, and J.-L. Pelouard, "Horizontal and vertical surface resonances in transmission metallic gratings," *J. Opt. A, Pure Appl. Opt.*, vol. 4, no. 5, pp. S154–S160, Sep. 2002.
[22] S. Tibuleac and R. Magnusson, "Reflection and transmission guided-mode resonance filters," *J. Opt. Soc. Amer. A, Opt. Image Sci.*, vol. 14, no. 7, pp. 1617–1626, Jul. 1997.
[23] J. Meier, J. Spitznagel, U. Kroll, C. Bucher, S. Fay, T. Moriarty, and A. Shah, "Potential of amorphous and microcrystalline silicon solar cells," *Thin Solid Films*, vol. 451/452, pp. 518–524, Mar. 2003.
[24] K. Kempa, M. J. Naughton, Z. F. Ren, A. Herczynski, T. Kirkpatrick, J. Rybczynski, and Y. Gao, "Hot electron effect in nanoscopically thin photovoltaic junctions," *Appl. Phys. Lett.*, vol. 95, no. 3, pp. 233121-1–233121-3, Dec. 2009.
[25] K. S. Cho, P. Mandal, K. Kim, I. H. Baek, S. Lee, H. Lim, D. J. Cho, S. Kim, J. J. Lee, and F. Rotermund, "Improved efficiency in GaAs solar cells by 1D and 2D nanopatterns fabricated by laser interference lithography," *Opt. Commun.*, vol. 284, no. 10/11, pp. 2608–2612, May 2011.
[26] W. Chen, M. D. Threson, S. Ishii, A. V. Kildishev, and V. M. Shalaev, "Ultra-thin ultra-smooth and low-loss silver films on a germanium wetting layer," *Opt. Exp.*, vol. 18, no. 5, pp. 5124–5134, Mar. 2010.